

# VIRTUAL PALEONTOLOGY – AN OVERVIEW

MARK SUTTON<sup>1</sup>, IMRAN RAHMAN<sup>2</sup>, AND RUSSELL GARWOOD<sup>3</sup>

<sup>1</sup>Department of Earth Sciences and Engineering, Imperial College London, London SW7 2BP, UK <m.sutton@imperial.ac.uk>

<sup>2</sup>Oxford University Museum of Natural History, Oxford OX1 3PW, UK

<imran.rahman@oum.ox.ac.uk>

<sup>3</sup>School of Earth, Atmospheric and Environmental Sciences, The University of Manchester, Manchester, M13 9PL, UK <russell.garwood@manchester.ac.uk>

ABSTRACT.—Virtual paleontology is the study of fossils through three-dimensional digital visualizations; it represents a powerful and well-established set of tools for the analysis and dissemination of fossil-data. Techniques are divisible into tomographic (i.e. slice-based) and surface-based types. Tomography has a long pre-digital history, but the recent explosion of virtual paleontology has resulted primarily from developments in X-ray computed tomography (CT), and of surface-based technologies such as laser scanning. Destructive tomographic methods include forms of physical-optical tomography (e.g. serial grinding); these are powerful but problematic techniques. Focused Ion Beam (FIB) tomography is a modern alternative for microfossils, also destructive but capable of extremely high resolutions. Non-destructive tomographic methods include the many forms of CT; these are the most widely used data-capture techniques at present, but are not universally applicable. Where CT is inappropriate, other non-destructive technologies (neutron tomography, magnetic resonance imaging, optical tomography) may prove suitable. Surface-based methods provide portable and convenient data capture for surface topography and texture, and may be appropriate when internal morphology is not of interest; technologies include

26 laser scanning, photogrammetry, and mechanical digitization. Reconstruction methods that  
27 produce visualizations from raw data are many and various; selection of an appropriate  
28 workflow will depend on many factors, but is an important consideration that should be  
29 addressed prior to any study. The vast majority of three-dimensional fossils can now be  
30 studied using some form of virtual paleontology, and barriers to broader uptake are being  
31 eroded. Technical issues regarding data-sharing, however, remain problematic. Technological  
32 developments continue; those promising tomographic recovery of compositional data are of  
33 particular relevance to paleontology.

34

35

## INTRODUCTION

### **What is Virtual Paleontology, and why is it needed?**

37 The term ‘virtual paleontology’ is used here in the sense of Sutton et al. (2014) – the study of  
38 fossils through three-dimensional digital visualizations (‘virtual fossils’), such as that shown  
39 in Fig. 1. Two-dimensional techniques that might be considered to be virtual paleontology  
40 tools also exist (e.g. Hammer et al., 2002), but in line with common usage we do not consider  
41 them here. For the sake of simplicity, our concept of virtual paleontology also excludes the  
42 manual construction of idealized virtual models of fossil taxa (e.g. Haug et al., 2012, fig. 11).  
43 Virtual paleontology, in our sense, therefore requires three-dimensionally preserved fossils.  
44 Whilst the compression of fossils onto a genuinely two-dimensional plane does occur, it is  
45 the exception; in most preservational scenarios at least an element of the original three-  
46 dimensionality is retained. These techniques are thus applicable (to some degree) to most  
47 paleontological material. Three-dimensional preservation retains more morphological  
48 information than true two-dimensional modes, but typically this information is problematic to  
49 extract. Many physical or chemical isolation/preparation methods exist (see e.g. Sutton,  
50 2008), but these are variously prone to specimen damage, loss of association between

51 disarticulated or weakly connected parts of fossils, issues with scaling to large or small  
52 specimen sizes, and inability to recover data from inside a fossil. Virtual paleontology can be  
53 thought of as a set of tools for more complete data-extraction from this sort of material.

54

55 The virtual paleontology approach, in addition to simple utility in data-extraction, also brings  
56 many novel advantages. Virtual specimens are typically more convenient to work with,  
57 requiring only a computer rather than expensive and lab-bound microscopes. They can be  
58 used for outreach and education (Rahman et al., 2012), and allow for virtual dissection and  
59 sectioning, where parts of the specimen can be isolated for clarity without risk of damage.

60 They allow for mark-up, typically in the form of color applied to discrete anatomical  
61 elements, which can greatly increase the ease of interpretation. They can be used as the basis  
62 for quantitative studies of functional morphology, such as finite-element analysis of stress  
63 and strain (e.g. Rayfield, 2007), or hydrodynamic flow modeling (e.g. Rahman et al., 2015).  
64 Finally, as virtual specimens are simply computer files, they can be easily copied and  
65 disseminated, facilitating collaborative analysis and publication.

66

### 67 **Tomography and surface-based virtual paleontology.**

68 A detailed taxonomy of virtual paleontology techniques is presented below, but the  
69 fundamental division of virtual paleontological data-capture techniques must be introduced at  
70 this stage. This is between (a) *tomography* and (b) *surface-based* techniques. Tomography is  
71 the study of three-dimensional structures through a series of two-dimensional parallel ‘slices’  
72 through a specimen (Fig. 2). In tomography, an individual slice-image is termed a *tomogram*,  
73 and a complete set of tomograms a *tomographic dataset*. Any device capable of producing  
74 tomograms is a *tomograph*; tomographs range from serial-grinding devices to sophisticated  
75 X-ray-based scanners. Surface-based techniques are those where the geometry of an external

76 surface is digitized in some fashion (e.g. laser scanning, photogrammetry); these do not  
77 involve slices, and do not capture data from the interior of a fossil.

78

## 79 **HISTORY OF VIRTUAL PALEONTOLOGY**

80 The history of virtual paleontology is relatively short when considered narrowly, but the use  
81 of its precursors and related methods is deep-rooted in the subject. The paleontological  
82 community has long appreciated the value of three-dimensional data and models, despite the  
83 difficulties in actually obtaining them using older methods, and the current explosion in  
84 virtual paleontology represents the satisfaction of a long-present hunger.

85

86 Virtual Paleontology, in the sense used here, originated in the early 1980s with X-ray  
87 computed tomography of vertebrate fossils. Tomography prior to digital visualization,  
88 however, has a long history. It was introduced to paleontology in the early 20th Century by  
89 the eccentric Oxford polymath William Sollas, who noted the utility of serial sectioning in  
90 biology and realized that serial grinding could provide similar datasets for paleontologists.  
91 His method (Sollas, 1903) utilized a custom-made serial-grinding tomograph capable of  
92 operating at 25  $\mu\text{m}$  intervals, photography of exposed surfaces, and manual tracing from glass  
93 photographic plates. Sollas applied his approach to a wide range of fossils; in the process he  
94 demonstrated the utility of tomography to a broad audience. He also described (Sollas, 1903)  
95 a physical-model visualization technique in which tomograms were traced onto thin layers of  
96 beeswax which were then cut out, stacked, and weakly heated to fuse them into a model. A  
97 similar though less aesthetically pleasing approach, using glued cardboard slices rather than  
98 fused wax, was also in early use and was probably also his invention. Sollas was primarily a  
99 vertebrate paleontologist, and it was in this field that his methods first became widely  
100 accepted, for instance in the seminal studies of Stensiö (1927) on the cranial anatomy of

101 Devonian fish. By the mid-20th Century, however, serial grinding had become a well-  
102 established technique, and was applied to many fossil vertebrates, invertebrates, and plants.  
103 Brachiopods provide an example of a group whose study was revolutionized by the  
104 technique; these invertebrates are often preserved three-dimensionally and articulated with  
105 valves firmly closed, concealing informative internal structures such as lophophore supports.  
106 Following the pioneering work of Muir-Wood (1934), the use of manually traced serial  
107 sections to document these structures has become almost ubiquitous.

108

109 A variety of serial-grinding tomographs have been used since Sollas's work (e.g. Croft, 1950;  
110 Ager, 1965; Sutton et al., 2001b), varying in terms of their complexity, degree of automation,  
111 maximum specimen size, and minimum grind-interval. Two variants on the technique that  
112 can mitigate its destructive nature have also been important. Firstly, acetate peels (see Galtier  
113 & Phillips, 1999) have been widely used as a means of data capture, especially but not  
114 exclusively in paleobotany. Peels, in some ways, are superior to photography of surfaces –  
115 they provide a permanent record of mineralogy and when stained can increase contrast  
116 between certain types of material. 'Peeling' is however ill-suited to modern visualization  
117 techniques (see below), and historical peel-datasets are thus often of limited utility. Secondly,  
118 serial sawing using fine saws (Kermack, 1970) became popular for larger (vertebrate) fossils  
119 in the late 20<sup>th</sup> Century; this approach retains original material, although at the cost of a  
120 reduction in inter-tomogram spacing.

121

122 All forms of tomography involving physical exposure of a surface and eventual optical  
123 imaging of that surface, whether with the intermediate of a peel and whether through  
124 photography or tracing, are grouped here as *physical-optical tomography* (sensu Sutton,  
125 2008).

126 While tomography was commonplace in the 20th Century, physical model-making (in wax,  
127 cardboard or any other material) became increasingly rare. Workers on particular groups (e.g.  
128 brachiopods) became sufficiently familiar with tomograms to be able to mentally visualize  
129 the data, and the benefits of being able to directly communicate these visualizations were  
130 perhaps overlooked. Reconstructions from tomographic data, where published, typically took  
131 the form of idealized pictorial or diagrammatic representations from such mentally-assembled  
132 models (e.g. the cupule reconstructions of Long, 1960); while aesthetically pleasing, this  
133 form of reconstruction lacked objectivity. However, as physical models were undoubtedly  
134 difficult to assemble, fragile, difficult to transport, and hard to work with, effective direct  
135 visualization had to await digital technology; this was not achieved for physical-optical data  
136 until the start of the 21st Century.

137

138 Tomography in paleontology has seen an enormous rise in uptake in recent years – Fig. 3  
139 provides a crude estimate of this, measured by the use of the term “tomography” in the  
140 paleontological literature; it shows a slow and steady rise, followed by a large upswing in the  
141 second half of the first decade of the 21<sup>st</sup> Century. This upswing primarily reflects the “CT  
142 revolution” (*sensu* Sutton et al., 2014); the increasing availability and popularity of X-ray CT.  
143 X-ray computed axial tomography (CT or CAT scanning) arose from medical radiography in  
144 the early 1970s. Early machines were limited in availability and resolution, so it was not until  
145 1982 that CT was first applied to vertebrate fossils (Tate and Cann, 1982). The first high-  
146 profile paleontological application was to *Archaeopteryx* (Haubitz et al., 1988). The growth  
147 of medical CT was accompanied by the development of three-dimensional digital  
148 visualization tools, of which early paleontological studies took advantage. Subsequently, the  
149 technology has become increasingly commonplace for the study of vertebrate fossils, which  
150 are often suitably-scaled for medical scanners. Serious CT study of smaller fossils began with

151 the advent of widely available X-ray microtomography (XMT /  $\mu$ CT) scanners, which can  
152 resolve features down to a few microns in size. The paleontological pioneers of micro-scale  
153 CT used high-resolution spiral CT (see Rowe et al., 2001; www.digimorph.org), but in the  
154 last 15 years XMT studies have proliferated, reflecting the increasing availability of relatively  
155 low-cost scanners. More recently, the advent of X-ray tomography beamlines at third-  
156 generation synchrotrons (see e.g. Donoghue et al., 2006; Tafforeau et al., 2006) has provided  
157 facilities for extremely high-resolution and high-fidelity CT study of fossils, including many  
158 intractable to lab-based XMT.

159

160 The CT revolution has hugely increased the uptake of tomography, but alongside it traditional  
161 physical-optical methods have enjoyed a limited renaissance, as for some material they  
162 remain the only practical means of data recovery. When married to modern digital  
163 photography, these methods can produce very high-fidelity data. Watters and Grotzinger  
164 (2001) provides an early example, applying these techniques to the Precambrian  
165 *Namacalathus*, but the most important example is the study of the invertebrate fossils of the  
166 Silurian Herefordshire Lagerstätte (see Briggs et al., 2008 for a summary), where an entire  
167 invertebrate fauna has been reconstructed via physical-optical tomography.

168

169 Pre-existing physical-optical datasets often consist of low-density (i.e. sparsely-spaced)  
170 tomograms. This drove early experimentation with vector surfacing (e.g. Chapman, 1989;  
171 Herbert, 1999) in which traced structures were connected and surfaced to produce relatively  
172 crude reconstructions; other idiosyncratic approaches to visualization were also trialled (e.g.  
173 Hammer, 1999). It was, however, the application of the 'mainstream' medical technique of  
174 isosurface-based rendering (see below) to high-density Herefordshire data by Sutton et al.  
175 (2001a, b) that first produced genuinely high-fidelity virtual models from physical-optical

176 data. This approach to visualization has been dominant since that study, although volume  
177 rendering (e.g. Hagadorn et al., 2006) and vector surfacing (e.g. Kamenz et al., 2008) have  
178 found occasional applications.

179

180 Other ‘niche’ approaches to paleontological tomography explored in recent years include  
181 magnetic resonance imaging (MRI), neutron tomography, optical tomography, and focussed  
182 ion beam (FIB) tomography. MRI is a routine medical scanning technology, but often  
183 performs poorly on solid materials. Applications have hence been rare (Mietchen et al., 2008,  
184 Clark et al., 2004). Neutron tomography utilizes neutron beams to perform tomography in a  
185 manner analogous to CT. Some studies have demonstrated limited utility, particularly in  
186 fossils preserving organic compounds or where the relatively weak absorption of neutrons by  
187 metal-rich rocks allows large and dense specimens to be imaged where X-rays fail (Schwarz  
188 et al., 2005; Winkler, 2006, Laaß & Schillinger, 2015). A relatively low resolution and  
189 limited availability have, however, militated against a broad uptake. Optical tomography  
190 (serial focusing – typically using confocal microscopy) is a very high-resolution non-  
191 destructive technique for data-capture from small translucent specimens. Confocal  
192 microscopy was first applied to fossils in the 1990s (e.g. Scott and Hemsley, 1991), but  
193 applications of optical tomography to fossils since have been sporadic (e.g. Ascaso et al.,  
194 2003; Kamenz et al., 2008). Finally, focussed ion beam (FIB) microscopes (see e.g. Phaneuf,  
195 1999) can use their beam to mill material at regular intervals, and can hence (laboriously)  
196 perform nano-scale tomography on fossils (e.g. Schiffbauer and Xiao, 2009; Wacey et al.,  
197 2012); this approach has seen rare but persistent application in recent years.

198

199 Surface-based techniques do not use tomography, but digitize the topography of the surface  
200 of a specimen, typically also capturing surface color. They provide a powerful approach

201 where the surface morphology represents the primary information of interest. Their history of  
202 usage is short. Mechanical digitization uses a ‘robotic’ arm equipped with sensors to record  
203 the position of a tip in 3-D space, and can hence collect surface points over an object. This  
204 approach was sporadically applied to vertebrate fossils in paleontology in the early 21st  
205 Century (Wilhite, 2003; Mallison et al., 2009), but has been superseded by non-contact  
206 approaches, i.e. laser scanning and photogrammetry. Laser scanning is a general term for a  
207 set of techniques where the reflection of a scanned laser-beam from a surface is used to  
208 record surface topography. The first portable scanners capable of rapid and precise scanning  
209 became available in the late 1990s, and have continued to improve since. Paleontological  
210 applications commenced with a study of part of a dinosaur skull (Lyons et al., 2000), and  
211 subsequently a flurry of work has used the approach on a broad range of fossils including  
212 vertebrates (Bates et al., 2009a), footprints (Bates et al., 2008, 2009b), and Ediacaran  
213 problematica (see e.g. Antcliff and Brasier, 2011). The technique is also in curatorial use for  
214 major museum-based digitization initiatives (e.g. GB3D, [www.3d-fossils.ac.uk](http://www.3d-fossils.ac.uk); the  
215 Smithsonian X 3D project, [www.3d.si.edu](http://www.3d.si.edu)). Photogrammetry is an alternative approach  
216 which assembles three-dimensional models from a set of two-dimensional photographs of an  
217 object. Analogue photogrammetry has a history, in cartography in particular (see e.g. Kraus,  
218 2007), and the widespread use of stereo-pairs to provide a form of three-dimensional model  
219 can also be seen as a forerunner of true photogrammetry-based virtual paleontology. Digital  
220 photogrammetry, which reconstructs models direct from digitally captured images, is now  
221 widely used in (for example) forensics and archaeology; and it has been shown to be at least  
222 as effective as laser scanning for some fossil materials (Falkingham, 2012). Paleontological  
223 applications began with reconstruction of dinosaur tracks (e.g. Breithaupt and Matthews,  
224 2001); while publications using it are still relatively scarce, it can be expected to become  
225 increasingly important in the near future.

226

227

## DATA CAPTURE METHODS

228

229

230

231

232

233

234

235

236

### **Destructive Tomography**

238

239

240

241

242

243

244

245

246

247

248

249

250

There are a great many approaches to 3-D data-capture available to paleontologists, and the vast majority of fossils will be amenable to at least one of these methods. Figure 4 provides a classification scheme for these (following Sutton et al., 2014). The most fundamental division is between surface-based and tomographic techniques (see above). Tomographic techniques are divided into destructive and non-destructive approaches, the former including traditional approaches such as serial grinding, and the latter encompassing scanning technologies such as CT. Surface techniques are divided into contact and non-contact categories. See Fig. 4 for further subdivisions.

This includes all forms of tomography which at least partially destroy the specimen in the production of the tomographic dataset. Tomograms are produced by physical exposure of a surface, which is then imaged in some way. The destructive nature of these methods is obviously undesirable; it can be seen as the conversion of a specimen from physical into digital form (rather than simple destruction), but this conversion process is never perfect. Data will be lost between tomograms, and no imaging technique can capture all information contained in an exposed surface; errors and mishaps are also unavoidable even where great care is taken. Destructive tomography always precludes the application of some future and potentially better data-extraction technique, and should thus be viewed as a last resort. Most destructive techniques are also time-consuming and labor-intensive; while equipment costs can be low, labor requirements can result in great expense. Additionally, destructively-gathered tomographic datasets typically require registration (alignment) of images prior to visualization (see below), which can also be time-consuming.

251

252 Despite these caveats, destructive techniques remain the best option for some fossils that are  
253 not easily amenable to non-destructive tomographic techniques. The fossils of the  
254 Herefordshire Lagerstätte (Briggs et al., 2008) provide just such an example; these show  
255 insufficient X-ray attenuation contrast for CT study, are too opaque for optical tomography,  
256 and are too small-scale for other techniques. Image capture of surfaces also facilitates data-  
257 rich imaging modes; color photography can capture subtleties of composition not evident in  
258 X-ray CT, and FIB techniques (see below) are capable of compositional, chemical, and  
259 crystallographic mapping of surfaces. Finally, some historical specimens have already been  
260 subjected to destructive physical-optical tomography; reconstruction using the existing data is  
261 here the only choice.

262

263 *Physical-optical tomography.*—

264 This term was introduced by Sutton (2008) to encompass a range of well-established  
265 destructive tomographic techniques; it is roughly equivalent to ‘serial sectioning’. It  
266 encompasses three approaches to serial exposure of tomographic surfaces.

267

268 Serial grinding (or lapping) is the most widely used approach. Specimens are positioned  
269 against an abrasive surface, motion is employed to physically grind away a small thickness of  
270 material (typically 10  $\mu\text{m}$ –1 mm). Details of methodology are many and various – see Sutton  
271 et al. (2001b, 2014) for one example. Equipment requirements can be as simple as a glass  
272 plate with abrasive powder, although more constrained grinding (and hence better  
273 reconstructions) require grinding-tomographs capable of removal of known thicknesses, and  
274 which guarantee that tomographic planes are parallel. Typically, these involve mounting  
275 specimens in an apparatus attached to a grinding wheel (see e.g. Croft, 1950; Ager, 1965),

276 and modern implementations typically make use of lapping machines intended for thin-  
277 section production (e.g. Sutton et al., 2014). Grinding-based tomography is maximally  
278 destructive and can be slow, especially for larger specimens, but can provide very closely  
279 spaced tomograms, and hence high-resolution reconstructions; structures as small as 10  $\mu\text{m}$   
280 are accessible. The grinding process also doubles as a polishing process, resulting in surfaces  
281 well suited for high-fidelity imaging.

282

283 Serial sawing exposes surfaces by cutting, preserving material in-between as wafers. Saws  
284 capable of fine cuts are preferable as they minimize the loss of material. Cheap fine-blade  
285 low-speed saws with a kerf under 0.4 mm are widely available and allow specimens to be  
286 clamped and precisely positioned; however, these can have high cut-times and are limited to  
287 specimens a few centimeters in size. Faster fine-blade saws (see e.g. Maisey, 1975) are  
288 expensive and also have size-restrictions. Wire saws (also expensive) have low kerfs and can  
289 cut large specimens, but single cuts can take hours. Reconstructions from serial-sawing data  
290 are complicated by the exposure of two (mirrored) surfaces by each cut, and the resulting  
291 inconsistent (alternating) inter-tomogram spacing. Sawing is fundamentally a lower-  
292 resolution technique than grinding methods, and does not produce surfaces that are as well  
293 polished. For these reasons, while occasionally used by vertebrate paleontologists, it has  
294 never been widely adopted. For large specimens not amenable to non-destructive tomography  
295 however, it may represent the only option.

296

297 Serial slicing involves serially removing and retaining fine slices of material with a  
298 microtome. The technique is widely used in biology and is capable of very high resolution,  
299 but is difficult with geological materials. Poplin and Ricqles (1970) described a variant  
300 applicable to fossils, but this is complex and laborious, and has only rarely been employed

301 (see e.g Kielan-Jaworowska et al., 1986). Modern high-precision ultramicrotomy can be  
302 carried out within a scanning electron microscope using dedicated equipment (see, e.g.  
303 Reingruber et al., 2011, Ma et al., 2016); this high-resolution technique might be appropriate  
304 for resin-mounted macerated fossils, but has yet to be trialled in paleontological research. All  
305 microtomy techniques, however, produce tomograms prone to image-distortions; these can  
306 degrade visualizations.

307

308 In physical-optical tomography, tomogram images are generated by photography or manual  
309 tracing. Direct digital photography of exposed surfaces is the preferred approach, using  
310 photographic techniques applicable to the specimen type and scale. See Sutton et al. (2014)  
311 for a full discussion. Cellulose acetate peels (or just ‘peels’) have been widely used as a  
312 means of producing a permanent record of fossil surfaces, for both physical-optical  
313 tomography and other purposes (see e.g. Galtier and Phillips, 1999). Serially-prepared peels  
314 can be scanned, photographed, or traced, and theoretically used for 3-D visualization.

315 However, even the best-prepared peels are prone to wrinkles, bubbles, tears stretches, and  
316 inconsistency of contrast, which render them very difficult to use for this purpose.

317 Interpretative tracings of structures, either direct from the surface or from photographs, can  
318 be used as an alternative input into visualization. These provide an effective means of  
319 cleaning difficult data, but may introduce ‘worker bias’, as well as complicating workflows.  
320 While historically important, this approach is now rarely used.

321

322 There are many pitfalls to be avoided when generating a physical-optical dataset for  
323 reconstruction. Importantly, reconstruction requires that all information within a tomographic  
324 image comes from a single plane; care must be taken that photography of translucent  
325 specimens or specimens with topography does not violate this requirement. Equally important

326 is the emplacement of fiduciary markings (e.g. vertical drilled holes) that can be used to  
327 guide registration (see below). See Sutton et al. (2014) for full discussion.

328

329 *Focused Ion Beam tomography (FIB)*.—

330 FIB is a lab-based tool for the imaging, milling, and deposition of material at the sub-  
331 micrometer scale, widely used in materials science and the semiconductor industry (Phaneuf,  
332 1999; Volkert and Minor, 2007). FIB machines can be used to sequentially mill and image  
333 specimens, and thus act as destructive tomographs for the study of structures as small as 5 nm  
334 (Uchic et al., 2007). Recent studies (Schiffbauer and Xiao, 2009, 2011; Wacey et al., 2012;  
335 Brasier et al., 2015) have demonstrated the paleontological utility of the technique, which can  
336 also theoretically provide data on the chemical/crystallographic structure of each tomogram if  
337 EDS (Energy-Dispersive X-ray Spectroscopy), EBSD (Electron Backscatter Diffraction) or  
338 SIMS (Secondary Ion Mass Spectrometry) detection is carried out. FIB is fully destructive  
339 and extremely time-consuming, with milling times per tomogram of up to an hour. Despite  
340 this, however, its extremely high resolution and potential to record compositional data render  
341 it a powerful tool.

342

### 343 **Non-destructive tomography**

344 A number of technologies exist which can create tomographic datasets, through interactions  
345 between electromagnetic radiation or subatomic particles and matter, without damaging the  
346 sample. This is desirable as it allows the sample to be subjected to future analyses, although  
347 note that there are rare situations in which non-destructive tomography can impact on future  
348 studies (Sutton et al., 2014), and that, for very high resolution work, sample preparation may  
349 be partially destructive. Non-destructive tomography is typically quick: most technologies  
350 acquire data in minutes to hours, and datasets are pre-registered (see below). There *are* fossils

351 which are not amenable to non-destructive approaches, but for many specimens they are  
352 effective tools; even where only partially effective, they represent a valuable initial approach.  
353 Numerous forms exist: X-ray computed tomography is the most widespread – in particular  
354 the high resolution form X-ray microtomography (XMT /  $\mu$ CT) – and is hence treated here in  
355 the greatest detail. Other approaches (including MRI, neutron tomography, confocal laser  
356 scanning microscopy, and optical tomography) have found more limited, but nevertheless  
357 important applications.

358

359 *Principles of CT.—*

360 All CT scans share the same principles: A large number of X-radiographs (=projections) of  
361 an object, collected at different angles, are used to compute a tomographic dataset (Abel et  
362 al., 2012). Approaches differ in detail between different forms of CT. In microtomography,  
363 where voxels (3D pixels) typically range between  $\sim 1 \mu\text{m}$  and  $\sim 100 \mu\text{m}$  in size, a sample is  
364 placed on a rotating manipulator between an X-ray source and a 2-D flat-panel detector (Fig.  
365 6). In contrast, medical, many industrial, and some high-resolution scanners rotate an X-ray  
366 source and detector around the object being scanned (Ketcham and Carlson, 2001).

367

368 Laboratory X-ray sources accelerate electrons (produced by heating a tungsten filament) into  
369 a target metal, where their deceleration creates a multi-wavelength ('polychromatic') X-ray  
370 beam, typically cone-shaped (Fig. 6A). Many samples are better imaged using a single  
371 wavelength ('monochromatic') beam of parallel X-rays, such as that created by a synchrotron  
372 (a form of particle accelerator; see Donoghue et al., 2006). Numerous algorithms for  
373 computing tomograms from projections exist; 'filtered back projection' is the most  
374 commonly encountered. The majority of tomographic datasets reconstructed in this manner  
375 are 3-D maps of X-ray attenuation within an object. X-ray attenuation is linked to the atomic

376 number and mass density variations within a sample, and thus can, in many samples,  
377 differentiate fossil from host sediment. A range of artifacts exist; see Sutton et al. (2014) for  
378 full discussion and mitigation strategies.

379

380 *Medical CT.—*

381 The source and detector in a medical CT scanner are placed on a rotating ‘gantry’; detectors  
382 in modern systems allow multiple slices to be collected simultaneously, and are hence rapid.  
383 The sample is placed on a mount/table, which is translated horizontally within the rotating  
384 gantry; these scanners are termed ‘spiral/helical’, reflecting the relative path of detector and  
385 specimen. Spatial resolution will typically be in the region of millimeters (although better  
386 resolution is attainable on specialized spiral scanners), but decimeter-scale fossils can be  
387 scanned provided the X-ray source is strong enough to penetrate the sample.

388

389 *Micro- and nanotomography.—*

390 Lab-based microtomography scanners (and nanotomography scanners, which can achieve  
391 higher resolution, e.g. through the use of optics) are typically designed for versatility, so have  
392 a large number of scanning options. Because the specimen is rotated within a cone beam (Fig.  
393 6A) and a flat-panel detector is used to collect projections (Fig. 6B), geometric magnification  
394 can be used – the closer a sample is to the source, the larger its radiograph appears on the  
395 detector panel. The current and voltage used to accelerate electrons, and hence the energy of  
396 the source’s X-rays, can also be modified. Attenuation of lower energies is more closely  
397 related to atomic number, providing greater contrast between materials. These X-rays can  
398 struggle to penetrate dense geological samples, and can thus produce ‘beam hardening’  
399 artifacts in which the centre of a scanned object appears artificially darkened; these artifacts  
400 complicate visualization. Polychromatic lab-based sources always emit some lower energy

401 X-rays that can cause beam hardening, but this problem can be addressed with filters – thin  
402 pieces of metal placed between the source and the sample to absorb lower energy X-rays.  
403 Lab-based CT scanning hence involves modifying the source voltage/current, and beam  
404 filtration, balancing the need for strong attenuation contrast with the need to avoid beam  
405 hardening. For a full overview of these considerations see Sutton et al. (2014). The process of  
406 scanning is otherwise relatively simple, requiring that the sample is stably positioned at the  
407 centre of rotation of the stage (mounting in florists' foam is a common approach), and that  
408 the exposure for each projection allows enough X-rays to penetrate the sample without  
409 saturating the detector panel outside the specimen. All scanners collect 'calibration images'  
410 to reduce artifacts from variations in detector sensitivity, and some possess additional optics  
411 to increase resolution. The technique can theoretically provide resolutions from tens of  
412 microns down to 50 nm with additional optics. Without optics, resolution is limited by the  
413 'spot size' size of the X-ray source, but resolution is also linked to the size of the object  
414 scanned: the sample should remain within the field of view throughout a 360° rotation. Thus  
415 for a 2000 x 2000 pixel detector, resolution will be 1/2000th the greatest dimension of the  
416 sample.

417

#### 418 *Synchrotron CT.*—

419 A synchrotron is a particle accelerator capable of producing a very high photon flux;  
420 synchrotrons have been widely used as intense X-ray sources in recent years. Scans are  
421 conducted on beamlines, and all beamlines differ in their precise characteristics. Very high  
422 resolution scanning is often referred to as synchrotron radiation X-ray tomographic  
423 microscopy (SRXTM; Donoghue et al., 2006). The key difference between tomography in a  
424 synchrotron and lab setting is that synchrotrons produce an intense, monochromatic, and  
425 parallel beam (Fig. 6C). This allows powerful optics to be used which can create very high

426 resolution datasets, although these lack geometric magnification (voxel size is constant  
427 irrespective of the sample to detector distance). In addition to attenuation, synchrotrons can  
428 create tomograms based on the phase shift of the X-ray beam, which relies on refraction  
429 within a sample. In samples with low attenuation contrast, such approaches can provide  
430 usable data. Resolutions vary between beamlines: minimum feature sizes in the order of tens  
431 of nanometers can be achieved, albeit with a concomitantly small field of view, whilst some  
432 beamlines can scan specimens several centimeters in size.

433

434 *Alternative forms of non-destructive tomography.—*

435 For specimens preserved in translucent rocks such as cherts, optical serial-focusing can  
436 recover usable tomographic data. This involves shining visible, UV, or IR light through a  
437 sample, and then recording tomograms using digital microscopy at different focal depths, to  
438 recover an image stack. Optical tomography can be achieved with conventional light  
439 microscopy (Kamenz et al., 2008), but here the inclusion of details outside the focal plane can  
440 complicate analysis. Hence, a commonly employed variant uses confocal laser scanning  
441 microscopy, an approach which concurrently images single focal planes, with out-of-focus  
442 light eliminated through the addition of a pinhole in the light path. This works best when  
443 samples autofluoresce, and has been applied to many chert-hosted fossils (Schopf and  
444 Kudryavtsev, 2009, Shi et al., 2013, Hickman-Lewis et al., in press).

445

446 Magnetic resonance imaging (MRI) has also found limited applications in paleontology (e.g.  
447 Clark et al., 2004): this uses strong magnetic fields to map the nuclei of some elements (often  
448 hydrogen) within a sample, and is capable of achieving resolutions in the region of 100  $\mu\text{m}$ .  
449 Whilst well-suited to biological samples, it is of limited utility in paleontology, and generally  
450 works well only when mapping water within crystalline phases (Mietchen et al., 2008).

451 Neutron tomography is similar in principle to X-ray-based tomography, but differs in that the  
452 incident radiation comprises neutrons, which attenuate based on interactions with the nuclei  
453 of a material (Winkler 2006). Attenuation from light atoms such as hydrogen is stronger than  
454 those with higher atomic numbers. This, coupled with higher penetration capabilities, makes  
455 neutron tomography a useful alternative for very large and/or dense samples (e.g. Schwarz et  
456 al., 2005), at a resolution of tens of micrometers. There has, however, been limited uptake in  
457 paleontology to date.

458

### 459 **Surface-based techniques**

460 Surface-based methods non-destructively capture the topography of an object in three  
461 dimensions; some also capture color data from that surface. Surface techniques tend to be  
462 inexpensive, accessible, non-destructive, and rapid; this combination renders them powerful  
463 weapons in the virtual paleontologist's armory. The collected datasets do not include details  
464 of the sample's interior, but the extent to which this is problematic will depend entirely on  
465 research goals. For many specimens already isolated from their matrix, surface capture may  
466 well be sufficient – vertebrate bones are an excellent example, and most applications of  
467 surface-based techniques have been in vertebrate paleontology.

468

#### 469 *Laser scanning.*—

470 Laser scanning is the most common surface-based technique employed today, both in  
471 paleontology and other fields. It uses a reflected laser beam to characterize the exterior 3-D  
472 shape and appearance of an object at distance. Laser scanning does not normally require  
473 sample preparation. Scanners range from hand-held devices for imaging small samples at  
474 sub-millimeter resolutions, to long-range systems capable of scanning larger field sites.  
475 Sutton et al. (2014) provide a detailed summary. If multiple scans are carried out for a single

476 specimen (e.g. to capture all surfaces of the object), the resulting point-clouds will need to be  
477 registered using computer software to obtain a complete 3-D reconstruction (see below). As  
478 an aid, reference objects such as spheres may need to be incorporated into the scanned  
479 scenes.

480

481 Triangulation-based scanners possess an angled sensor offset from the laser source, and use  
482 position of reflection-impact on this sensor to determine target range through triangulation.  
483 Full object coverage is achieved by automatic scanning of the beam across the surface, and/or  
484 movement of the object, for example by rotation on a stage. A variety of instruments exist,  
485 capable of resolutions approaching 50  $\mu\text{m}$  and/or ranges of up to a few meters. Triangulation  
486 scanners often perform poorly in bright sunlight, but are suitable for laboratory use; they have  
487 been used to study many centimeter-scale fossils including Ediacaran organisms (e.g.  
488 Antcliffe and Brasier, 2011), insects (e.g. Béthoux et al., 2004), trace fossils (e.g. Platt et al.,  
489 2010), and vertebrates (e.g. Zhang et al., 2000).

490

491 Time-of-flight scanners use pulsed lasers and precise timing of received reflections to  
492 calculate distance-to-target from the traversal-time of light. The beam is scanned over a  
493 surface (typically using a system of rotating mirrors); data-point capture rates are typically  
494 tens of thousands per second. Scanners are ‘luggable’ and often tripod-mounted; they can  
495 operate at ranges of 1 km or more, and image at resolutions down to a few millimeters. They  
496 are tolerant of outdoor conditions, and are ideal for field applications such as dinosaur  
497 trackway studies (e.g. Bates et al., 2008), as well as reconstruction of large vertebrate  
498 skeletons (e.g. Bates et al., 2009a).

499

500 Phase-shift scanners are similar to time-of-flight scanners, but measure distance by  
501 modulating beam power and comparing the phase of the reflection. Their capabilities are  
502 similar to those of time-of-flight scanners, although their range is an order of magnitude  
503 lower and their capture-rate an order of magnitude higher. Paleontological applications have  
504 been limited to a few field studies of assemblages (e.g. Haring et al., 2009).

505

506 *Photogrammetry.*—

507 Photogrammetry determines surface topography from multiple two-dimensional photographs  
508 acquired from different viewpoints. It is widely used in cartography, medicine, forensics, and  
509 archaeology. It requires only basic and highly portable equipment: a digital camera for data  
510 capture, and a computer with appropriate software for reconstruction. High-quality  
511 reconstructions require consistent lighting conditions and a large number of images (typically  
512 over 100), but the quality of the camera is not critical. Reconstruction of a point-cloud from  
513 images is now generally automated, and can be achieved with open-source software. Recent  
514 studies have shown that photogrammetry is capable of producing reconstructions of  
515 paleontological material with similar or better resolutions (i.e. denser point clouds) than many  
516 laser scanners (Remondino et al., 2010; Falkingham, 2012). The method is scale-less, and so  
517 is theoretically applicable to surfaces of any size; very small specimens are amenable to SEM  
518 photogrammetry (e.g. Kearsley et al., 2007), although no paleontological work has yet been  
519 published using this variant. Applications to date have primarily documented dinosaur  
520 skeletons (e.g. Stoinski, 2011) and track-sites (e.g. Bates et al., 2009b), but the technique has  
521 great potential for broader uptake.

522

523 *Mechanical digitization.*—

524 Mechanical or contact digitization uses a mechanical arm with rotational/positional sensors at  
525 each joint, and a digitizing tip. The tip is moved manually over the surface of a specimen, and  
526 its position in three dimensions is recorded by the sensors. The technique has been used for  
527 the collection of landmark data for morphometric studies (e.g. Green and Alemseged, 2012),  
528 but also as a data-capture methodology for virtual paleontology; Mallison et al. (2009)  
529 provide full documentation and a workflow. Digitization accuracy under ideal conditions can  
530 reach 50  $\mu\text{m}$  (manufacturer's data, [www.3d-microscribe.com](http://www.3d-microscribe.com)), and Mallison et al. (2009)  
531 reported accuracy was close to 1 mm for a 200 mm specimen. The method is relatively cheap,  
532 and data-capture time is normally low. Resultant datasets and reconstructions are also small,  
533 facilitating their dissemination, storage, and visualization. However accuracy is lower than  
534 that of laser scanning and photogrammetry, and surface color is not captured. Additionally,  
535 there is a small risk of damage to specimens from contact with the digitizing tip and the need  
536 to emplace markings (see Mallison et al., 2009). The method is best suited to large and robust  
537 specimens with relatively simple morphology; for these reasons, paleontological applications  
538 to date have focused on isolated vertebrate bones.

539

#### 540 **Summary of data-capture methods**

541 The methods detailed above differ in many ways, and selection of the most appropriate can  
542 be daunting. Figure 5 provides a summary of scales of operation and other key aspects of  
543 methods, and is provided as an aid to selection; a more complete guide is provided by Sutton  
544 et al. (2014). Method selection will in practice need to take into account factors such as the  
545 properties of the specimen to be studied (e.g. X-ray contrast, scale, translucency), availability  
546 of and familiarity with equipment, degree of concern over specimen-damage, and financial  
547 restrictions.

548

549  
550  
551  
552  
553  
554  
555  
556  
557  
558  
559  
560  
561  
562

## RECONSTRUCTION AND VISUALIZATION METHODS

Raw captured data can sometimes be visualized directly and with minimum user-intervention by software bundled with the capture-device. This will, however, rarely provide an optimal model, and in many cases no such facility will be available. An understanding of the methods and workflows required for visualization is hence important. Figure 7 summarizes the stages through which data may pass from capture to an output model suitable for study. A typical methodology will generate a triangle-mesh model, as these provide maximal flexibility in terms of model-production and data-interchange. However there are many possible routes and workflows, and selection should be based on the type of input data, preparation requirements, software availability, and the use to which the final model will be put. Software will, in all cases, be required; detailed discussion of available packages is beyond the scope of this review, except to note that both commercial and free packages exist. SPIERS (Sutton et al., 2012) is an example of a free software-suite for tomographic reconstruction and visualization.

### Reconstruction of tomographic data

#### *Registration.—*

A registered tomographic dataset is one where the tomograms are correctly aligned (registered) with respect to one another, such that objects do not ‘jump around’ when the tomogram sequence is viewed in order. Reconstruction of un-registered datasets is not possible, and imperfect registration degrades models. Some data-capture techniques naturally provide registered data; these include optical tomography, CT, neutron tomography, and MRI (CT and neutron tomography require conversion of data from raw attenuation images to registered computed tomograms, but this is normally performed just after acquisition by the scanner software). Physical-optical and FIB datasets are typically un-registered.

573 Registration of datasets is a discrete reconstruction step that precedes all others. It comprises  
574 the digital translation, rotation, and sometimes rescaling of tomograms, to ensure that correct  
575 alignment is achieved. Registration is greatly facilitated by the presence of ‘fiduciary  
576 markings’ such as drilled holes or edges (see Sutton et al., 2014) in the tomograms; these  
577 allow the correct position of a tomogram to be deduced by ensuring that the markings are in  
578 the same position in each image. In their absence, the morphology of the specimen itself is  
579 the only guide to registration, and this is fraught with difficulties. Registration requires  
580 dedicated software, and can be manual, automatic, or semi-automatic (automatic followed by  
581 manual fine-tuning). Our experience is that automatic registration can only be relied upon for  
582 unusually ‘clean’ datasets; in most cases, manual or semi-automatic registration will be  
583 necessary, and this can be time-consuming.

584

585 *Isosurfacing.*—

586 The most commonly used reconstruction workflows treat a tomographic dataset as a  
587 ‘volume’, and involve the calculation of an ‘isosurface’ to represent the specimen. A volume  
588 is the 3-D equivalent of a pixel-based (raster) image, comprising a three-dimensional grid of  
589 equally sized 3-D volume elements (voxels) instead of a two-dimensional grid of pixels.  
590 Voxels, like pixels, each represent a single measurement of color, attenuation, or simply  
591 brightness. A registered tomographic dataset with regular tomogram spacing does not need  
592 ‘conversion’ into a volume; it is a conceptual shift. An isosurface is a three-dimensional  
593 surface connecting all points of a constant intensity within the volume. With a correctly  
594 determined ‘threshold’ level (i.e. color/brightness-based cut-off), the isosurface will follow  
595 the boundary of the specimen under study; the provision of visual-feedback tools to aid in  
596 this determination is a key function of reconstruction software. Isosurfaces are usually  
597 generated using the marching cubes algorithm (Lorenson and Cline, 1987), which produces a

598 triangle-mesh dataset (see below) defining the isosurface or isosurfaces – there is no  
599 requirement for all points to connect into a single surface. The marching cubes algorithm is  
600 robust and well understood, but for high-resolution datasets it can produce surfaces with a  
601 prohibitively high triangle-count, potentially hundreds of millions or more. Mesh-  
602 simplification algorithms can help mitigate this issue (see Sutton et al., 2014), but are not a  
603 panacea; simplification or noise-reduction prior to isosurface reconstruction is often  
604 necessary, either through virtual preparation (see below), or by reducing tomogram  
605 resolution.

606

607 *Vector surfacing.*—

608 Vector surfacing (*sensu* Sutton et al., 2014) involves the manual or semi-automatic tracing of  
609 structures of interest in each tomogram, normally in the form of closed loops defined as  
610 spline curves. Stacked two-dimensional splines from multiple tomograms are used to  
611 generate a mathematically defined three-dimensional surface, typically in the form of a  
612 triangle mesh. This historically important approach produces low triangle-count models, and  
613 can produce ‘smoother’ outputs than isosurface-based approaches where inter-tomogram  
614 spacing is high and/or inconsistent. It is also not sensitive to variations (e.g. in lighting or  
615 quality) between tomograms; requiring only that a tracing can be made. In general, it  
616 performs well for simple objects such as individual vertebrate bones, but not for complex  
617 objects that merge and split between tomograms. Vector surfacing remains viable, but has  
618 become an uncommon approach in recent years (though see e.g. Maloof et al., 2010), as  
619 appropriate software is rare and the method is time-consuming, requiring an extra  
620 interpretation stage. For datasets with a high tomogram frequency (e.g. from scanners), it has  
621 no particular advantages beyond reduction of triangle-count.

622

623           *Virtual preparation.*—

624 Volume data can be reconstructed ‘raw’, but in most cases isosurface-based reconstructions  
625 are greatly improved by preparation work, the virtual equivalent of the manual preparation  
626 work traditionally employed to physically expose specimens. Preparation involves either  
627 modifying voxel-values by brightening or darkening them (see e.g. Sutton et al., 2001),  
628 applying masks/labels to split the final model into discrete parts or regions-of-interest (see  
629 e.g. Abel et al., 2012; Sutton et al., 2012), or refining visualization rules in an attempt to  
630 improve discrimination. Depending on the capabilities of the software used, volume  
631 preparation can be carried out either in two dimensions, on a tomogram-by-tomogram basis,  
632 or in three dimensions; the latter approach is generally faster, but the former more precise.  
633 Virtual preparation is a time-consuming and skilled task, but can greatly increase the fidelity  
634 and scientific value of any resulting visualization. Note that preparation, particularly in terms  
635 of the application of masks/labels, is also applicable to direct volume rendering (see below).

636

637   **Reconstruction of surface-based data.**

638 Laser scanning and photogrammetry (see above) typically generate data in the form of ‘point  
639 clouds’, a series of points in three-dimensional space for which a position (and often a color)  
640 is recorded. Mechanical digitization may either generate point clouds or spline curves  
641 suitable for vector-surfacing (see above).

642

643 Point-cloud data for an object often comprises several point-cloud datasets, resulting from the  
644 need to scan objects from different angles, or to use multiple scan-stations to ensure full  
645 coverage. The process of fusing these datasets into one is normally termed registration (not to  
646 be confused with tomographic registration, see above). Registration is achieved via  
647 identification of correspondences between separate datasets, enabling their relative positions

648 to be determined; it is normally carried out automatically or semi-automatically by software  
649 associated with the acquisition device.

650

651 Point clouds can be directly visualized (see below), or can be surfaced through triangulation  
652 algorithms to produce a triangle mesh. The latter approach allows conversion of the model  
653 into a similar format to that produced by other virtual paleontological workflows and  
654 increases the range of visualization options. It is, however, not computationally  
655 straightforward; while effective algorithms exist (see e.g. Salman et al., 2010), they are still  
656 the subject of active research, and not always integrated into reconstruction software.

657

## 658 **Visualization**

659 Visualization is the final stage of reconstruction, where data is converted into a model that  
660 can be studied directly, either through on-screen manipulation and viewing, or as a physical  
661 model. Triangle-mesh data, the most common form, is treated in the most detail.

662

### 663 *Visualization of triangles meshes.—*

664 Modern graphics-hardware is heavily optimized for visualizing triangle-mesh objects, and  
665 hence even modest computers are capable of very fast rendering of datasets of this type. This  
666 fit of hardware to data provides a compelling reason to convert data to this format where  
667 possible; while hardware-accelerated rendering can produce static images, its real power lies  
668 in interactive visualization systems where fast rendering speeds allow the user to manipulate  
669 a virtual model, rotating, zooming, and altering visibility of discrete elements at will.

670 Powerful workstation-class computers allow even very large datasets to be studied in this  
671 way, but the degree to which interactive viewing is practical depends on the efficiency of the  
672 software as well as the speed of the hardware.

673 Triangle-mesh datasets are often processed (‘filtered’) prior to visualization. Filters may for  
674 instance be used to decrease triangle count, to smooth out blockiness, or to remove  
675 disconnected ‘islands’. Such filters modify data, so should be used with care – see Sutton et  
676 al. (2014) for more detail.

677

678 Triangle-mesh models can also be visualized using slower but more photorealistic techniques  
679 such as ray-tracing; this approach is recommended for the production of high-quality static  
680 images or pre-rendered animations for publication. Triangle meshes are also amenable to 3-D  
681 printing, a term which encompasses a set of techniques for the production of a physical three-  
682 dimensional object from a digital model. 3-D printed models are typically inferior to virtual  
683 models for research purposes, but are well suited to the communication of results to non-  
684 specialist audiences (see e.g. Rahman et al., 2012).

685

686 *Direct volume rendering.*—

687 Methods exist for the direct visualization of volume data, obviating the need for isosurface  
688 calculation (see e.g. Lichtenbelt et al., 1998). These vary in detail and in computational  
689 efficiency, but all directly project a volume onto a 2-D image without producing a triangle-  
690 mesh, via a ‘transfer function’ that determines a color to be displayed from the density of (or  
691 gradient between) voxels. These approaches cope well with specimens in which gradations  
692 are present, as no arbitrary thresholding is required, automatically implement translucency of  
693 structures, and can visualize any color information in the original volume. Results can rival  
694 triangle-mesh visualizations aesthetically. However, rendering speeds are normally  
695 substantially slower than those for triangle-mesh datasets, and rendering requires the presence  
696 of the full volume dataset, which can hamper both visualization on less-powerful hardware  
697 and data-sharing. Software availability is a further limiting factor, although the *Drishti*

698 package ([sf.anu.edu.au/Vizlab/drishti/](http://sf.anu.edu.au/Vizlab/drishti/)) provides a free solution. Likely for these reasons,  
699 uptake in paleontology has been limited (though see e.g. Schiffbauer and Xiao, 2009; Albani  
700 et al., 2010).

701

702 *Direct point-cloud rendering.*—

703 The direct rendering of point-cloud data from surface-based capture techniques is  
704 straightforward; points are simply projected from three into two dimensions, and drawn as  
705 small colored squares or circles in the appropriate position. Direct point-cloud rendering is  
706 normally less visually appealing than triangle-mesh based rendering and often slower, as it is  
707 less amenable to hardware acceleration. However, it avoids the non-trivial triangulation step  
708 (see above) and is hence simpler to achieve. For dense point clouds, it may be an adequate  
709 means to visualize surface data, and where points are sparse it has the benefit of making this  
710 sparsity clear to the viewer.

711

## 712 **CHALLENGES AND DEVELOPMENTS**

713 Virtual paleontology is now firmly established as an important tool, or more properly set of  
714 tools, for the study and dissemination of paleontological specimens. The vast majority of  
715 three-dimensionally preserved fossils can now be successfully studied using some form of  
716 virtual paleontology, and the advantages to the approach are now widely understood.  
717 Nonetheless, there are still barriers to the further and faster uptake of these methods.  
718 One such barrier is the ‘difficulty’ of these methods, both perceived and actual. The  
719 increasing availability of reconstruction software, the improved visibility of the techniques,  
720 and the increasing number of publications describing methods are actively combating this  
721 problem. Nonetheless, virtual paleontology can be an expensive and time-consuming  
722 undertaking, and like all techniques, should only be deployed where benefits outweigh costs.

723 Perhaps the greatest potential in virtual paleontology lies in improved data-availability for  
724 researchers. Fossil data underlying paleontological research has always been available via  
725 museum repositories of specimens, but the logistical difficulties hamper routine re-study of  
726 material. Virtual specimens are (in theory) far easier to access. The dissemination of three-  
727 dimensional morphological data underlying ‘virtual paleontology’ publications is clearly  
728 desirable in the interests of scientific clarity, as well as to facilitate further research on the  
729 specimens (see e.g. Callaway, 2011). Just as gene-sequence data is routinely made available  
730 to all interested parties via GenBank ([www.ncbi.nlm.nih.gov/genbank](http://www.ncbi.nlm.nih.gov/genbank)), with immeasurable  
731 benefits for genetic science (Strasser, 2008), the routine publication of virtual fossil data  
732 would be hugely beneficial for the science of paleontology. While such data releases are  
733 becoming increasingly common, they are still far from ubiquitous. This may partly reflect a  
734 reluctance amongst researchers to ‘give away’ data without guarantee of reciprocation  
735 (Sutton et al., 2012), but technical impediments are also an issue. Virtual paleontological data  
736 can take many different forms depending on the approach used (Fig. 7), can reach very large  
737 file-sizes, and there is no agreement as to exactly which data constitutes ‘the specimen’ (e.g.  
738 raw tomograms? prepared tomograms? triangle-mesh models?). There is also no agreement  
739 as to which file format should be used for any particular data type (though see Sutton et al.,  
740 2012), or indeed as to which of the many existing online repositories should be preferred.  
741 Sutton et al. (2014) provide a more in-depth discussion of these problems, which remain  
742 obstructive to the development of the science.

743

744 The techniques available for virtual paleontology have changed radically in the last 20 years.  
745 Most techniques, for instance, have seen improvements in resolution; these improvements are  
746 likely to continue. The importance of non-destructive (scanning) methods is likely to  
747 continue to increase, as the necessary equipment becomes increasingly available at a lower

748 cost. Nonetheless, destructive methods will continue to find niche applications, especially  
749 FIB tomography, which provides the highest resolution of any method discussed. Surface-  
750 based techniques have seen a rapid increase in paleontological usage in recent years, and the  
751 increasing availability of photogrammetry is likely to drive further uptake; attractions of this  
752 approach include its scale-agnostic nature, high portability, and very low equipment costs.

753

754 While other tomographic methods will continue to have some applications, X-ray computed  
755 tomography (CT) is likely to remain the mainstay of virtual paleontology; access costs should  
756 continue to fall, and resolution and availability continue to increase. Developments in phase-  
757 contrast methods (at synchrotrons and also with lab sources) are already greatly increasing  
758 the resolving power of CT for difficult (i.e. low attenuation-contrast) specimens.

759 Additionally, the development of new methods capable of mapping elemental or  
760 mineralogical composition in three dimensions are of great potential significance; color CT is  
761 perhaps the most exciting of these. These methods are still experimental and/or prohibitively  
762 time consuming (Sutton et al., 2014), but should they become practical we predict a very  
763 significant paleontological uptake.

764

765 Virtual paleontology is no longer a niche undertaking; these techniques are now at the core of  
766 the discipline. Their ongoing development will only continue to increase their importance in  
767 the future.

768

## 769 ACKNOWLEDGEMENTS

770 Imran Rahman was supported by an 1851 Royal Commission Research Fellowship. We also  
771 thank the Paleontological Society for support of this short course.

772

773 REFERENCES

- 774 Abel, R. L., C. Laurini, and M. Richter. 2012. A palaeobiologist's guide to "virtual"micro-CT  
775 preparation. *Palaeontologia Electronica*, 15:6T, 17p.
- 776 Ager, D. V. 1965. Serial Grinding Techniques, p, 212–224. *In* B. Kummel and D. Raup  
777 (eds.), *Handbook of Palaeontological Techniques*, Freeman, San Fransisco.
- 778 Albani, A.E, S. Bengtson, D. E. Canfield, A. Bekker, P. Macchiarelli, A. H. Mazurier, E. U.  
779 Hammarlund, P. Boulvais, J-J. Dupuy, C. Fontaine, F. T. Fürsich, F. Gauthier-Lafaye, P.  
780 Janvier, E. Javaux, F. O. Ossa, A.-C. Pierson-Wickmann, A. Riboulleau, P. Sardini, D.  
781 Vachard, M. Whitehouse, and A. Meunier. 2010. Large colonial organisms with coordinated  
782 growth in oxygenated environments 2.1 Gyr ago. *Nature*, 466:100–104.
- 783 Antcliffe, J.B. and M. D. Brasier. 2011. Fossils with little relief: using Lasers to conserve,  
784 image, and analyse the Ediacara biota, p. 223–240. *In* M. Laflamme, J. D. Schiffbauer, and S.  
785 Q. Dornbos, (eds.), *Quantifying the Evolution of Early Life: Numerical Approaches to the*  
786 *Evaluation of Fossils and Ancient Ecosystems*. Springer, Dordrecht.
- 787 Ascaso, C., J. Wierzchos, J. C. Corral, R. López, and J. Alonso. 2003. New applications of  
788 light and electron microscopic techniques for the study of microbiological inclusions in  
789 amber. *Journal of Paleontology*, 77:1182–1192.
- 790 Bates K. T., F. Rarity, P. L. Manning, D. Hodgetts, B. Vial, O. Oms, A. Galobart, and R. L.  
791 Gawthorpe. 2008. High-resolution LiDAR and photogrammetric survey of the Fumanya  
792 dinosaur tracksites (Catalonia): implications for the conservation and interpretation of  
793 geological heritage sites. *Journal of the Geological Society of London*, 165:115–127.
- 794 Bates K. T., P. L. Manning, D. Hodgetts, and W. I. Sellers. 2009a. Estimating mass  
795 properties of dinosaurs using laser imaging and 3D computer modelling. *PLoS ONE*,  
796 4(2):e4532.
- 797 Bates, K.T., B. H. Breithaupt, P. L. Falkingham, N. Matthews, D. Hodgetts, and P. K.  
798 Manning. 2009b. Integrated LiDAR and photogrammetric documentation of the Red Gulch  
799 dinosaur tracksite (Wyoming, USA), p. 101–103. *In*: S. E. Foss, J. L. Cavin, T. Brown, J. I.  
800 Kirkland, and V. L. Santucci (eds.), *Proceedings of the Eighth Conference on Fossil*  
801 *Resources*, Utah Geological Survey, Salt Lake City.

802 Béthoux, O., J. McBride, and C. Maul. 2004. Surface laser scanning of fossil insect wings.  
803 *Palaeontology*, 47:13–19.

804 Brasier, M. D., J. Antcliffe, M. Saunders and D. Wacey. 2015. Changing the picture of  
805 Earth's earliest fossils (3.5–1.9 Ga) with new approaches and new discoveries. *PNAS*  
806 112:4859–4864.

807 Breithaupt, B. H. and N. A. Matthews, N. A. 2001. Preserving paleontological resources  
808 using photogrammetry and geographic information systems, p. 62–70. *In*: Harmon, D. (ed.)  
809 *Crossing Boundaries in Park Management: Proceedings of the 11th Conference on Research*  
810 *and Resource Management in Parks and Public Lands*. The George Wright Society, Hancock.

811 Briggs, D. E. G., David J. Siveter, Derek J. Siveter, and M. D. Sutton. 2008. Virtual fossils  
812 from a 425 million-year-old volcanic ash. *American Scientist*, 96:474–481.

813 Callaway, E. 2011. Fossil data enter the web period. *Nature*, 472:150.

814 Chapman, R. E. 1989. Computer assembly of serial sections, p. 157–164. *In* M. Feldmann,  
815 M., R. Chapman, and J. T. Hannibal (eds.), *Paleotechniques*. Special Publication 4,  
816 *Paleontological Society*, Boulder.

817 Clark, N. D. L., C. Adams, T. Lawton, A. R. Cruickshank, and K. Woods. 2004. The Elgin  
818 marvel: using magnetic resonance imaging to look at a mouldic fossil from the Permian of  
819 Elgin, Scotland, UK. *Magnetic Resonance Imaging*, 22:269–273.

820 Croft, W. N. 1950. A parallel grinding instrument for the investigation of fossils by serial  
821 sections. *Journal of Paleontology*, 24:693–698.

822 Donoghue, P. C. J., S. Bengtson, X. Dong, X., N. J. Gostling, T. Huldtgren, J. A.  
823 Cunningham, C. Yin, Z. Yue, F. Peng, and M. Stampanoni. 2006. Synchrotron X-ray  
824 tomographic microscopy of fossil embryos. *Nature*, 442:680–683.

825 Falkingham, P. L. 2012. Acquisition of high resolution 3D models using free, open-source,  
826 photogrammetric software. *Palaeontologia Electronica*, 15(1):1T.

827 Galtier, J. and T. Phillips. 1999. The acetate peel technique, p. 67–70. *In* T. P. Jones and N.  
828 P. Rowe (eds.), *Fossil Plants and Spores*, The Geological Society, London.

829 Green, D. J. and Z. Alemseged. 2012. *Australopithecus afarensis* scapular ontogeny,  
830 function, and the role of climbing in human evolution. *Science*, 338:514–517.

831 Hagadorn, J. W., S. Xiao, S., P. C. J. Donoghue, S. Bengtson, N. J. Gostling, M. Pawlowska,  
832 E. C. Raff, R. A. Raff, E. R. Turner, Y. Chongyu, C. Zhou, X. Yuan, M. B. McFeely, M.  
833 Stampanoni, and K. H. Nealson. 2006. Cellular and Subcellular Structure of Neoproterozoic  
834 Animal Embryos. *Science*, 314:291–294.

835 Hammer, Ø. 1999. Computer-aided study of growth patterns in tabulate corals, exemplified  
836 by *Catenipora heintzi* from Ringerike, Oslo Region. *Norsk Geologisk Tidsskrift*, 79:219–  
837 226.

838 Hammer, Ø., S. Bengtson, T. Malzbender, T. and D. Gelb. 2002. Imaging fossils using  
839 reflectance transformation and interactive manipulation of virtual light sources.  
840 *Palaeontologia Electronica*, 5 (4), 9A.

841 Haring, A., U. Exner, and M. Harzhauser, M. 2009. Surveying a fossil oyster reef using  
842 terrestrial laser scanning. *Geophysical Research Abstracts*, 11:10714.

843 Haubitz, B., M. Prokop, W. Doehring, J. H. Ostrom, and P. Wellnhofer. 1988. Computed  
844 tomography of Archaeopteryx. *Palaeobiology*, 14:206–213.

845 Haug, J. T., D. E. G. Briggs, and C. Haug, 2012. Morphology and function in the Cambrian  
846 Burgess Shale megacheiran arthropod *Leanchoilia superlata* and the application of a  
847 descriptive matrix. *BMC Evolutionary Biology*, 12:162.

848 Herbert, M. J. 1999. Computer-based serial section reconstruction, p. 93–126. *In* D. A. T.  
849 Harper (ed.), *Numerical Palaeobiology: Computer-Based Modelling and Analysis of Fossils*  
850 *and their Distributions*. Wiley, Chichester.

851 Hickman-Lewis, K., R. J. Garwood, M. D. Brasier, N. McLoughlin, T. Goral, H. Jiang, and  
852 D. Wacey, *In press*. Carbonaceous microstructures of the 3.46Ga stratiform ‘Apex chert’,  
853 Chinaman Creek locality, Pilbara, Western Australia. *Precambrian Research*.

854 Kamenz, C., J. A. Dunlop, G. Scholtz., H. Kerp, and H. Hass. 2008. Microanatomy of Early  
855 Devonian book lungs. *Biology Letters*, 4:212–215.

856 Kearsley, A. T., M. J. Burchell, G. A. Graham, F. Hörz, P. A. Wozniakiewicz, and M. J.  
857 Cole. 2007. Cometary dust characteristics: comparison of stardust craters with laboratory  
858 impacts. 38th Lunar and Planetary Science Conference, 1562.

859 Kermack, D. M. 1970. True serial-sectioning of fossil material. *Biological Journal of the*  
860 *Linnean Society*, 2:47–53.

861 Ketcham, R. A., and W. D. Carlson. 2001. Acquisition, optimization and interpretation of X-  
862 ray computed tomographic imagery: applications to the geosciences. *Computers &*  
863 *Geosciences*, 27:381–400.

864 Kielan-Jaworowska, Z., R. Presley, and C. A. Poplin. 1986. The Cranial Vascular System in  
865 Taeniolabidoid Multituberculate Mammals. *Philosophical Transactions of the Royal Society*  
866 *of London. Series B, Biological Sciences*, 313:525–602.

867 Kraus, K. 2007. *Photogrammetry: Geometry from images and laser scans* (2nd edition).  
868 Walter de Gruyter, Berlin.

869 Laaß, M. and B. Schillinger. 2015. Reconstructing the Auditory Apparatus of Therapsids by  
870 Means of Neutron Tomography. *Physics Procedia*, 69:628–635.

871 Lichtenbelt, B., R. Crane, and S. Naqvi. 1998. *Introduction to volume rendering*. Prentice  
872 Hall, Upper Saddle River, NJ.

873 Long, A. G. 1960. *Stamnostoma huttonense* gen. et sp. nov., a pteridosperm seed and cupule  
874 from the Calciferous Sandstone series of Berwickshire. *Transactions of the Royal Society of*  
875 *Edinburgh*, 64:201–215.

876 Lorenzen, W.E. and H. E. Cline. 1987. Marching Cubes: A high resolution 3D surface  
877 construction algorithm. *Computer Graphics*, 21:163–169.

878 Lyons, P. D, M. Rioux, and R. T. Patterson, R.T. 2000. Application of a three-dimensional  
879 color laser scanner to paleontology: an interactive model of a juvenile *Tylosaurus* sp.  
880 basisphenoid-basioccipital. *Palaeontologia Electronica*, 3(2):4A.

881 Ma, L., K. G. Taylor, P. D. Lee, K. J. Dobson, P. J. Dowey, and L. Courtois. 2016. Novel 3D  
882 centimetre-to nano-scale quantification of an organic-rich mudstone: The Carboniferous  
883 Bowland Shale, Northern England. *Marine and Petroleum Geology*, 72:193–205.

884 Maisey, J. G. 1975. A serial sectioning technique for fossils and hard tissues. *Curator*,  
885 18:140–147.

886 Mallison, H., A. Hohloch,, and H. Pfretzschner. 2009. Mechanical digitizing for paleontology  
887 – new and improved techniques. *Palaeontologia Electronica*, 12(2):4T.

888 Maloof, A. C., C. V. Rose, R. Beach, B. M. Samuels, C. C. Calmet, D. H. Erwin, G. R.  
889 Poirer, N. Yao, and F. J. Simons. 2010. Possible animal-body fossils in pre-Marinoan  
890 limestones from South Australia. *Nature Geoscience*, 3:653–659.

891 Mietchen, D., M. Aberhan, B. Manz, O. Hampe, B. Mohr, C. Neumann, and F. Volke. 2008.  
892 Three-dimensional magnetic resonance imaging of fossils across taxa. *Biogeosciences*, 5:25–  
893 41.

894 Muir-Wood, H. M. 1934. On the Internal Structure of Some Mesozoic Brachiopoda.  
895 *Philosophical Transactions of the Royal Society of London. Series B*, 223(494–508):511–  
896 567.

897 Phaneuf, M.W. 1999. Applications of focused ion beam microscopy to materials science  
898 specimens. *Micron*, 30:277–288.

899 Platt, B. F., S. T. Hasiotis, and D. R. Hirmas. 2010. Use of low-cost multistripe laser  
900 triangulation (MLT) scanning technology for three-dimensional quantitative  
901 paleoichnological and neoichnological studies. *Journal of Sedimentary Research*, 80:590–  
902 610.

903 Poplin, C. A. M. Ricqles, de. 1970. A technique of serial sectioning for the study of  
904 undecalcified fossils. *Curator*, 13:7–20.

905 Rahman, I.A., K. Adcock, K. and R. J. Garwood. 2012. Virtual fossils: a new resource for  
906 science communication in paleontology. *Evolution: Education and Outreach*, 5:635–641.

907 Rahman, I. A., S. Zamora, P. L. Falkingham, P.L., and J. C. Phillips. 2015. Cambrian cinctan  
908 echinoderms shed light on feeding in the ancestral deuterostome. *Proceedings of the Royal  
909 Society B*, 282:20151964.

910 Rayfield, E. J. 2007. Finite Element Analysis and Understanding the Biomechanics and  
911 Evolution of Living and Fossil Organisms. *Annual Review of Earth and Planetary Sciences*,  
912 35:541–576.

913 Reingruber, H., A. Zankel, P. Mayrhofer, and P. Poelt. 2011. Quantitative characterization of  
914 microfiltration membranes by 3D reconstruction. *Journal of Membrane Science*, 372:66-74.

915 Remondino, F., A. Rizzi, S. Girardi, F. M. Petti, and M. Avanzini. 2010. 3D ichnology—  
916 recovering digital 3D models of dinosaur footprints. *The Photogrammetric Record*, 25:266–  
917 282.

918 Rowe, T. B., M. Colbert, R. A. Ketcham, J. Maisano, and P. Owen, P. 2001. High-resolution  
919 X-ray computed tomography in vertebrate morphology. *Journal of Morphology*, 248: 277–  
920 278.

921 Salman, N., M. Yvinec, and Q. Merigot. 2010. Feature preserving mesh generation from 3D  
922 point clouds. *Computer Graphics Forum*, 29:1623–1632.

923 Schiffbauer, J. D. & S. Xiao. 2009. Novel application of focused ion beam electron  
924 microscopy (FIB-EM) in preparation and analysis of microfossil ultrastructures: a new view  
925 of complexity in early eukaryotic organisms. *Palaios*, 24:616–626.

926 Schiffbauer, J. D. & S. Xiao. 2011. Paleobiological applications of focused ion beam electron  
927 microscopy (FIB-EM): an ultrastructural approach to the (micro)fossil record. p. 321–354. *In*  
928 M. Laflamme, J. D. Schiffbauer and S.Q. Dornbos (eds.), *Quantifying the Evolution of Early*  
929 *Life: Numerical Approaches to the Evaluation of Fossils and Ancient Ecosystems*. Springer,  
930 Dordrecht. Schopf, J. W. and A. B. Kudryavtsev. 2009. Confocal laser scanning microscopy  
931 and Raman imagery of ancient microscopic fossils. *Precambrian Research*, 173:39–49.

932 Schwarz, D, P. L. Vontobel, H. Eberhard, C. A. Meyer, and G. Bongartz, G. 2005. Neutron  
933 Tomography of Internal Structures of Vertebrate Remains: A Comparison with X-ray  
934 Computed Tomography. *Paleontologia Electronica*, 8(2):30A.

935 Scott, A.C. and A. R. Hemsley. 1991. A comparison of new microscopical techniques for the  
936 study of fossil spore wall ultrastructure. *Review of Palaeobotany and Palynology*, 67:133–  
937 139.

938 Shi, C. S., J. W. Schopf, and A. B. Kudryavtsev. 2013. Characterization of the stem anatomy  
939 of the Eocene fern *Dennstaedtiopsis aerenchymata* (Dennstaedtiaceae) by use of confocal  
940 laser scanning microscopy. *American Journal of Botany*, 100:1626–1640.

941 Sollas, W. J. 1903. A method for the investigation of fossils by serial sections. *Philosophical*  
942 *Transactions of the Royal Society of London*, B, 196(214–224):259–265.

943 Stensiö, E. A. 1927. The Downtonian and Devonian vertebrates of Spitzbergen. *Skrifter om*  
944 *Svalbard og Nordishavet*, 12, 391 p.

945 Stoinski, S. 2011. From a skeleton to a 3D dinosaur, p. 147–164. *In* A. M. T. Elewa (ed.),  
946 *Computational Paleontology*. Springer, Berlin.

947 Strasser, B. J. 2008. GenBank – Natural History in the 21st Century? *Science*, 322:537–538.

948 Sutton M. D., Briggs, D. E. G., David J. Siveter, and Derek J. Siveter. 2001a. An  
949 exceptionally preserved vermiform mollusc from the Silurian of England. *Nature*, 410: 461–  
950 463.

951 Sutton, M. D., D. E. G. Briggs, David J. Siveter, and Derek J. Siveter. 2001b. Methodologies  
952 for the Visualization and Reconstruction of Three-dimensional Fossils from the Silurian  
953 Herefordshire Lagerstätte. *Palaeontologia Electronica*, 4(1):1A.

954 Sutton, M. D, R. J. Garwood, David J. Siveter, and Derek J. Siveter. 2012. SPIERS and  
955 VAXML; A software toolkit for tomographic visualisation, and a format for virtual specimen  
956 interchange. *Palaeontologia Electronica* 15(2):14.

957 Sutton, M. D., I. A. Rahman, and R. J. Garwood, R.J. 2014. *Techniques for Virtual*  
958 *Palaeontology*. Wiley-Blackwell, 208 p.

959 Sutton, M. D. 2008. Tomographic techniques for the study of exceptionally preserved fossils.  
960 *Proceedings of the Royal Society B*, 275:1587–1593.

961 Tafforeau, P., R. Boistel, E. Boller, A. Bravin, M. Brunet, Y. Chaimanee, P. Cloetens, M.  
962 Feist, J. Hosszowska, J-J. Jaeger, R. F. Kay, V. Lazzari, L. Marivaux, A. Nel, C. Nemoz, X.  
963 Thibault, P. Vignaud, and S. Zabler. 2006. Applications of X-ray synchrotron  
964 microtomography for non-destructive 3D studies of paleontological specimens. *Applied*  
965 *Physics A*, 83:195–202.

966 Tate, J. R. and C. E. Cann. 1982. High-resolution computed tomography for the comparative  
967 study of fossil and extant bone. *American Journal of Physical Anthropology*, 58:67–73.

968 Uchic, M. D., L. Holzer, B. J. Inkson, E. L. Principe, and P. Munroe. 2007. Three-  
969 dimensional microstructural characterization using focused ion beam tomography. *MRS*  
970 *Bulletin*, 32:408–416.

971 Volkert, C.A. & A. M. Minor. 2007. Focused ion beam microscopy and micromachining.  
972 *MRS Bulletin*, 32:389–399.

973 Wacey, D., S. Menon, L. Green, D. Gerstmann, C. Kong, N. Mcloughlin, M. Saunders, and  
974 M. Brasier. 2012. Taphonomy of very ancient microfossils from the ~3400 Ma Strelley Pool  
975 Formation and ~1900 Ma Gunflint Formation: New insights using a focused ion beam.  
976 *Precambrian Research*, 220–221:234–250.

977 Watters, W. A. and J. P. Grotzinger. 2001. Digital reconstruction of calcified early  
978 metazoans, terminal Proterozoic Nama Group, Namibia. *Paleobiology*, 27:159–171.

979 Wilhite, R. 2003. Digitizing large fossil skeletal elements for three-dimensional applications.  
980 *Palaeontologia Electronica*, 5(2):4A.

981 Winkler, B. 2006. Applications of Neutron Radiography and Neutron Tomography. Reviews  
982 in Mineralogy and Geochemistry, 63:459–471.

983 Zhang, G., Y. Tsou, and A. L. Rosenberger, A.L. 2000. Reconstruction of the Homunculus  
984 skull using a combined scanning and stereolithography process. Rapid Prototyping Journal,  
985 6:267–275.

986

987

988

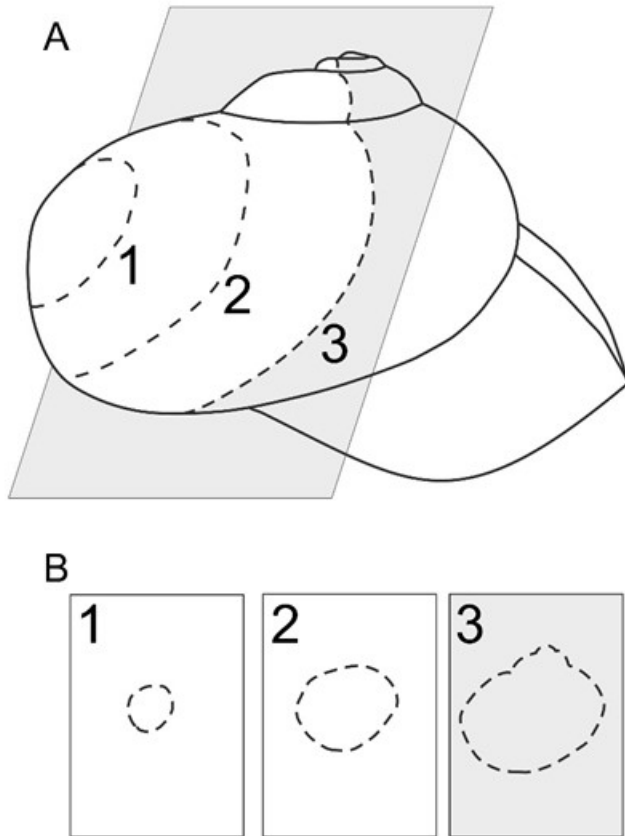
989 FIGURES AND CAPTIONS



990

991 FIGURE 1.— An example of a virtual fossil. *Offacolus kingi*, OUMNH C.29557, from the  
992 Silurian Herefordshire Lagerstätte, UK. Scale bar = 1 mm.

993



994

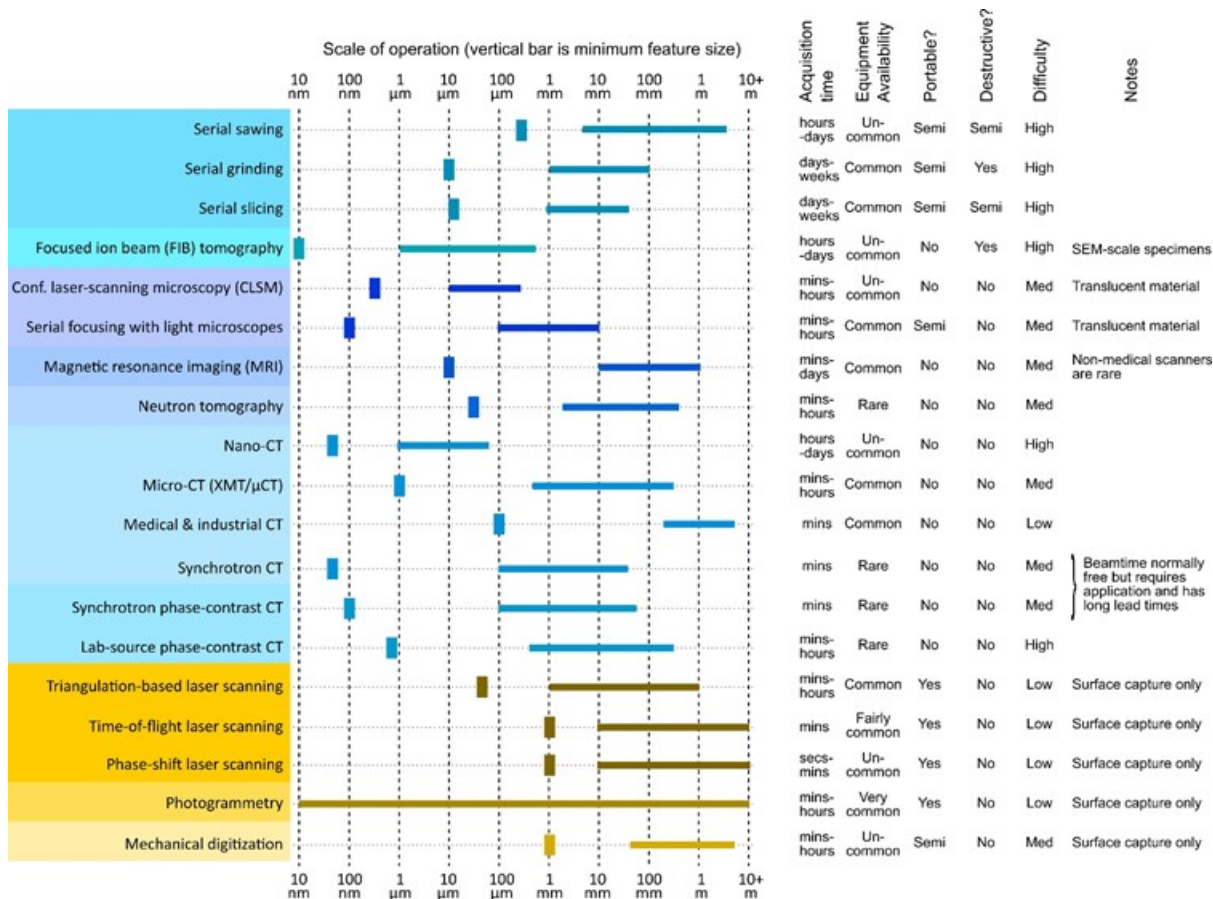
995 FIGURE 2.— Tomography – 3-D reconstruction using a series of two-dimensional slices.

996 Idealized example (after Sutton, 2008, fig. 1). (A) Three parallel and evenly spaced serial

997 tomograms (1–3) through an idealized gastropod fossil; (B) Resultant tomographic dataset.

998

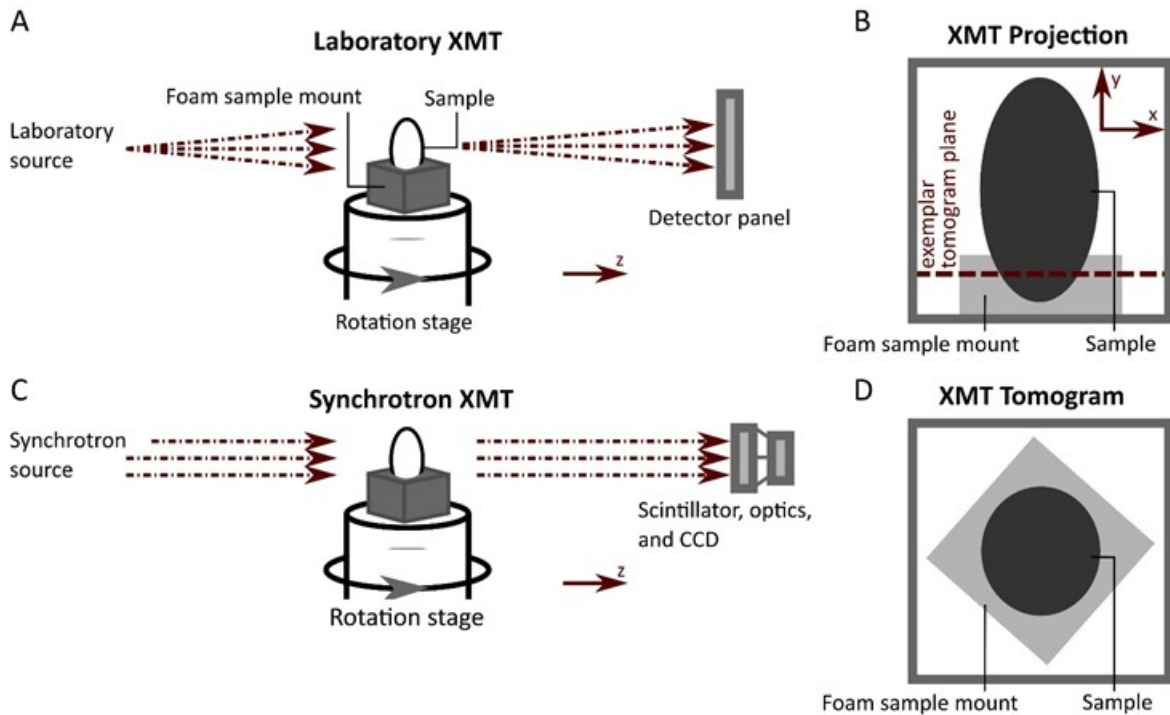




1009

1010 FIGURE 5.— Comparison of methodologies by scale and other important qualities  
 1011 (simplified from Sutton et al., 2014, fig. 7.3 and table 7.1). For scale, thick lines represent  
 1012 approximate range of feature-of-interest sizes, and vertical bars represent approximate  
 1013 minimum resolvable feature size. Note that photogrammetry is scale-agnostic; the minimum  
 1014 size given (for SEM photogrammetry) is notional. Other data are largely indicative guides.  
 1015 Note that semi-destructive approaches are those where some material is destroyed, but the  
 1016 majority is retained; portable equipment can be easily carried by a single person, potentially  
 1017 into the field, while semi-portable equipment is ‘luggable’ from one laboratory to another;  
 1018 difficulty is a qualitative estimate of how complex and challenging the entire procedure will  
 1019 be to a relative novice; complications with visualization are included in the estimate, as are  
 1020 likely degrees of technical support available.

1021

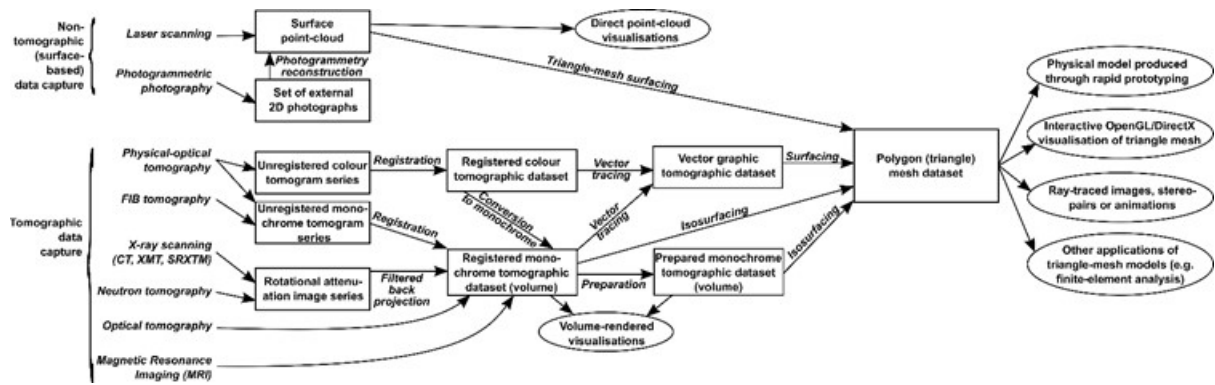


1022

1023 FIGURE 6.— Comparison of different forms of X-ray computed tomography. (A) A  
 1024 laboratory-based X-ray microtomography setup, showing a sample mounted in florists foam  
 1025 on a rotation stage. Of note is the cone beam configuration providing geometric  
 1026 magnification. (B) An X-ray projection of the sample from panel (A), with a plane marked on  
 1027 which will be reconstructed as a tomogram. (C) A possible synchrotron-based X-ray  
 1028 microtomography setup. The beam is parallel, and magnification is provide by optics behind  
 1029 a scintillator, which fluoresces on exposure to X-rays. (D) An exemplar tomogram, based on  
 1030 the exemplar tomogram plane in panel (B).

1031

1032



1033  
 1034 FIGURE 7.— Common reconstruction workflows. Rectangles; data-set types generated  
 1035 during the reconstruction process. Ellipses; outputs (visualizations, models, etc.). Unbounded  
 1036 text at top; inputs. Modified from Sutton et al. (2012, fig. 2). Reproduced with permission of  
 1037 The Palaeontological Association.

1038

1039